

THE BRIGHT SHARC SURVEY SELECTION FUNCTION AND ITS IMPACT ON THE CLUSTER X-RAY LUMINOSITY FUNCTION: COSMOLOGICAL APPLICATIONS



C. Adami, M. Ulmer, A. Romer, R. Nichol, B. Holden, R. Pildis
LAM Marseille, NU Evanston, CMU Pittsburgh, UC Chicago

We present the results of a comprehensive set of simulations designed to quantify the selection function of the Bright SHARC survey (Romer et al. 2000a) for distant clusters. The statistical significance of the simulations relied on the creation of thousands of artificial clusters with redshifts and luminosities in the range $0.25 < z < 0.95$ and $0.5 < L_X < 10 \times 10^{44} \text{ erg s}^{-1}$ (0.5–2.0 keV). We created 1 standard and 19 varied distribution functions, each of which assumed a different set of cluster, cosmological and operational parameters. The parameters we varied included the values of Ω_0 , Ω_Λ , β , core radius (r_c) and ellipticity (e). We also investigated how non-standard surface brightness profiles (i.e the Navarro, Frenk & White 1997, NFW, model); and cooling flows, influence the selection function in the Bright SHARC survey. For our standard set we adopted the parameters used during the derivation of the Bright SHARC Cluster X-ray Luminosity Function (CXLF, Nichol et al. 1999, N99), i.e. $\Omega_0 = 1$, $\Omega_\Lambda=0$ and an isothermal β model with $\beta=0.67$, $r_c=250 \text{ kpc}$ and $e = 0.15$. We found that certain parameters have a dramatic effect on our ability to detect clusters, e.g. the presence of a NFW profile or a strong cooling flow profile, or the value of r_c and β . Other parameters had very little effect, e.g. the cluster ellipticity. We show also that all the tested parameters have only a small influence on the computed luminosity of the clusters (*recovered luminosity* in the text) except the presence of a strong cooling flow. We stress the importance of cluster follow-up, by *Chandra* and XMM, in order to better constrain the morphology of the distant clusters found in the Bright SHARC and other surveys.

1 Introduction

Numerous authors have demonstrated that the observed evolution of clusters of galaxies can place a strong constraint on the present day value of the matter density of the Universe, $\rho_0/\rho_c=\Omega_m$ (see Gunn & Gott 1972; Press & Schechter 1974; Lacey & Cole 1993; Oukbir & Blanchard 1992 & 1997; Richstone, Loeb & Turner 1992). In recent years, there has been considerable interest in constraining Ω_m using the observed abundance of clusters as a function of redshift (see Viana & Liddle 1996 & 1999; Henry et al. 1997; Bahcall, Fan & Cen 1997; Sadat et al. 1998; Reichart et al. 1999; Borgani et al. 1999). The effect of Ω_0 ($=\Omega_m$ if $\Omega_\Lambda=0$) on cluster abundances is very large. For example, the space density of high redshift ($z > 0.3$), massive ($T > 6 \text{ KeV}$) clusters in an $\Omega_m = 0.3$ universe is 100 times greater than that in an $\Omega_m = 1$ universe (e.g. Viana & Liddle 1996, Oukbir & Blanchard 1992, Oukbir & Blanchard 1997, Romer et al. 2000b). Unfortunately, the various studies performed to date have produced

a wide range of results, from $\Omega_m = 0.3 \pm 0.1$ (Bahcall et al. 1997) to $\Omega_m = 0.96_{-0.32}^{+0.36}$ (Reichart et al. 1999). This observed dispersion in Ω_m is most likely due to the fact that the cluster surveys currently available do not sample a large enough volume to include sufficient numbers of distant and massive clusters. Nevertheless, it is still important to quantify the uncertainties that are applicable to the data in hand. This allows us not only better to understand the uncertainties in using the ROSAT database, but this also provides insight as how to proceed in the future.

In this contribution, we discuss the selection function of one of the ROSAT archival surveys for distant clusters; namely, the Bright Serendipitous High-redshift Archival ROSAT Cluster (Bright SHARC) survey. We describe the results of a full set of simulations designed to determine the ability of the Bright SHARC survey to detect clusters of different morphologies, luminosities and redshifts under different cosmological and observational conditions. Earlier works such as that of Rosati et al. (1995) or Vikhlinin et al. (1998) set the standards of this kind of work, however, we have performed these simulations in a much more detailed way and have examined the effects of different cosmologies and cluster profiles on the completeness of the Bright SHARC survey.

Throughout we keep H_0 fixed at $50 \text{ km s}^{-1} \text{ Mpc}^{-1}$ but Ω_m , Ω_Λ ($=\Lambda c^2/3H_0$) and Ω_0 are varied.

2 Survey Overview

The Bright SHARC survey has been described in detail in Romer et al. (2000a: R00 hereafter), but we review the salient points here. The survey was comprised of 460 ROSAT PSPC pointings. The pointings all had exposure times greater than 10 ks and lie at Galactic latitudes greater than $b = |20^\circ|$. The Bright SHARC survey took advantage of the fact that the pointing targets covered only a small fraction of the total field of view of the PSPC detector, leaving the rest of the field of view (FOV) available for serendipitous cluster detections. FOV of the ROSAT PSPC extends to a radius of $\simeq 1^\circ$, but in the Bright SHARC survey, we chose to use only an annular region bounded by radii of 2.'5 and 22.'4. (Beyond 22.'4 the point spread function degrades rapidly which makes detections of the extended emission from clusters increasingly difficult.)

Each of the 460 pointings was run through a pipeline processing which identified the extended sources in each field. In total 374 extended sources were catalogued (see Appendix E of R00). These 374 sources met the following three criteria; they were detected at a signal-to-noise ratio of 8 or higher, they were more than 3σ (wavelet defined, see R00) extended and had filling factors^a of less than $f = 1.3$. The Bright SHARC survey is comprised of the brightest 94 of these 374 extended sources. These 94 all have count rates in excess of $0.01163 \text{ counts s}^{-1}$. Optical identifications have been secured for all but 3 of the Bright SHARC sources, resulting in a sample of 37 clusters ($0.3 < z < 0.83$: 12 clusters).

3 Simulation Process

The simulation procedure is quite complex and we describe it below in detail, but, in essence, the basic concept is straightforward. We have created thousands of artificial clusters with a range of different parameters, placed these clusters at different positions in ROSAT PSPC pointings and then ran the modified pointings through the Bright SHARC survey pipeline processing. We used these simulations to tell us how sensitive the survey is to each type of artificial cluster and also to evaluate the completeness of the SHARC survey as a function of X-ray luminosity, shape and cosmology.

^aThe filling factor is a simple shape parameter designed to filter out obviously blended sources, see R00

3.1 Effect of the Cosmological Parameters

We tested the effect of the underlying cosmological models on our ability to detect clusters by comparing the results of run 1 ($\Omega_m=1$) with the results of runs 2 ($\Omega_m=0.1$, $\Omega_\Lambda=0$) and 3 ($\Omega_m=0.4$, $\Lambda=0.6$). For both the alternative cosmologies tested, we found lower values of the *Bright SHARC detection efficiency*. This was because, for the same redshift and total luminosity, a low Ω_m produced clusters which were larger in angular extent than did a high $\Omega_m = 1$. Despite their increased angular extent, clusters in a low Ω_m Universe are harder to detect than their counterparts in a $\Omega_m = 1$ Universe because their surface brightness (and hence contrast against the X-ray background) is diminished.

For those artificial clusters detected in runs 2 and 3 we find their *recovered luminosities* to be similar to those measured in run 1. The mean percentage difference between the *recovered luminosities* in run 1 and run 2 was $3\pm 18\%$. This difference was $7\pm 30\%$ when compared runs 1 and 3. The standard errors associated with these two mean percentages are somewhat large, but we did not detect any systematic trends with the redshift and/or the luminosity.

In summary, if we assume lower values of Ω_0 (for a flat or an open Universe), the luminosity estimates are as good, on average, as when we assume $\Omega_0=1$ ($\Omega_\Lambda = 0$). However, changing the value of Ω_0 and Ω_Λ has a marked effect on the detection efficiency of the survey, especially for high redshift and/or low luminosity clusters. This effect has, however, only a small influence on the derived Cluster X-ray Luminosity Function because of the distribution of the Bright SHARC real clusters in the (z, L_{44}) space.

3.2 Effect of the ellipticity

We have investigated the effect of cluster ellipticity on the detection efficiency of the survey by comparing the results from run 1 ($e = 0.15$) to those from runs 4 ($e = 0.0$) and 5 ($e = 0.3$). For a fixed cosmology, an elliptical cluster will have a higher central surface brightness than a circular cluster of the same luminosity in proportion of the surface difference induced by the ellipticity (if the image is contracted along the minor axis). In doing this, we kept the core radius constant along the major axis: we contracted the image along the minor axis. Instead, we could have elongated the image along the major axis to make clusters elliptical. However, doing this would lead to a lower surface brightness cluster. Such clusters would be similar to our low- β and our large core radius models. We find no systematic trend in the *Bright SHARC detection efficiency*. We find no systematic trend in the *recovered luminosity* with ellipticity. The mean percentage difference in *recovered luminosity* is $1\pm 22\%$ between runs 1 and 4 and $2\pm 30\%$ between runs 1 and 5. This is good, since it shows that the R00 luminosity method, which assumes a single ellipticity of $e = 0$, did not introduce a systematic bias into the measured Bright SHARC cluster luminosities.

In summary, ellipticity has minimal effect on the *recovered luminosity* and on the *Bright SHARC detection efficiency*.

3.3 Effect of the Central Surface Brightness Model

Here we examine how the adopted surface brightness model for the artificial clusters affects their detectability. In run 1 a simple isothermal β -profile was used. We contrast this with a pseudo-NFW profile in run 6 and with a pseudo cooling flow profile in runs 7 and 8. Both the NFW profile and the cooling flow profiles are more peaked than the isothermal β -profile, and hence, they have higher central surface brightnesses. The detection efficiency for a moderate cooling flow (run 7) was similar to that for run 1 and there are no clear trends with redshift or luminosity. In other words, the presence of a moderate cooling flow does not have a significant impact on the detectability of a cluster. By contrast, the strong cooling flows (run 8) and the

NFW profile clusters simulated in run 6 were significantly (up to two times) easier to detect than the equivalent isothermal β -profile clusters. We attribute this to the surface brightness in the cluster core being significantly higher than for a β -profile.

We found the *recovered luminosities* from runs 6 and 7 to be very similar to those from run 1. The mean percentage difference in *recovered luminosity* is $2\pm 17\%$ between runs 1 and 6 and $2\pm 16\%$ between runs 1 and 7. This demonstrates that the R00 methodology, which assumes all clusters have isothermal β -profiles, provides a valid approximation for the run 6 and 7.

The *recovered luminosities* from run 8 are, however, underestimated by $27\pm 7\%$. Based on the uncertainty, this trend is significant. Assuming that the R00 methodology is able to recover a valid luminosity for β -like profiles, we can infer that the difference comes mainly from the cooling-flow profile itself. If the Gaussian model peak of the cooling-flow is relatively bright compared to the β -profile (200 kpc in this case), the R00 methodology fails to recover the entire luminosity due to the normalization technique which assumed a standard β -profile.

However, the percentages of clusters exhibiting strong cooling flows in the Bright SHARC redshift range is probably low. Assuming, for example, a central cooling-time between 1 and 2 Gyears (e.g. Peres et al. 1998), most of the known cooling-flows in clusters at $z\sim 0.1$ have been initiated only at redshifts lower than $z\sim 0.3$ ($q_0 \leq 0.5$). It is, therefore, very likely that we only have a small percentage of cooling-flow clusters (or at least with moderate cooling flows) in the redshift range of our simulations and in the Bright SHARC. This is confirmed by the fact that there are not many clusters detected at redshift higher than 0.3 with known cooling-flows (e.g. 3C 295; Henry & Henriksen 1986) whereas the X-ray detection of such clusters should be easier, theoretically, than for the non-cooling-flow clusters.

3.4 Effect of β

In runs 9 and 10 we examined the effects of β on the detectability of clusters with isothermal β -profiles. In run 9 we use a value of $\beta=0.55$, whereas, in run 10, we use $\beta=0.75$. We compared the results from these runs against those from run 1 ($\beta=0.67$). Clusters with higher Beta values are easier to detect. This can be explained by the fact that higher β values result in more concentrated, and hence higher surface brightness, clusters.

Lowering the value of β to $\beta=0.55$ was found to have a significant effect on value of the *recovered luminosity*. Where the detection is easy (low redshift + high luminosity), the *recovered luminosity* estimate is the same whatever the value of β . Where the detection is more difficult, however, the *recovered luminosity* of the $\beta=0.55$ tends to be low. There are two reasons for this. First the detection efficiency for $\beta=0.55$ clusters is significantly lower than that of $\beta=0.67$ clusters. So that, even when the run 1 detection efficiency is above our minimum threshold of 15%, the run 9 efficiency can be much lower. (In other words well into the regime where most of the detections are spurious.) Second the R00 luminosity method, which assumes all clusters have $\beta=0.67$, breaks down when $\beta < 0.67$. If the true β value is smaller than $\beta=0.67$, this aperture will encircle less than 80% of the actual flux, which can lead to a significant underestimate of the total luminosity. In principle, R00 could have corrected for the β effect by fitting the cluster profiles and then deriving a flux, but the low number of counts available in the ROSAT PSPC images made such an approach impractical. We found that the fitted β value was so poorly constrained as to lead to best fit values that could easily be very far away from the true value.

3.5 Effect of the Core Radius

In runs 11 and 12 we examined the effects of the size of the core radius (r_c) on the detectability of clusters. In run 11 we adopted $r_c = 100$ kpc and, in run 12, we adopted $r_c = 400$ kpc. We compared the results from these runs with those from run 1 ($r_c = 250$ kpc). The effect of r_c turns out to be more complex than the effect of β . The *Bright SHARC detection efficiencies*

for the $r_c = 100$ kpc clusters was consistently lower than that of $r_c = 250$ kpc clusters, with the effect being most pronounced at lower luminosities. By contrast, the $r_c = 400$ kpc clusters could be either easier or harder to detect than the $r_c = 250$ kpc clusters, depending on the redshift and luminosity. They were easier to detect in the low redshift $L_{44} = 2.0$ and the intermediate redshift $L_{44} = 5.0$ bins, but harder to detect in the $L_{44} = 10.0$ and low redshift $L_{44} = 5.0$ bins. This demonstrates the competing effects of surface brightness and extent: Clusters with higher surface brightnesses were easier for the wavelet pipeline to detect, but those with small angular sizes were less likely to be flagged as extended sources.

We found no significant difference in the *recovered luminosity* between run 11 ($r_c=400$ kpc) and run 1 ($r_c=250$ kpc). By comparison, we found a small, but systematic, enhancement in the *recovered luminosity* for run 11 ($r_c=100$ kpc) compared to run 1 ($r_c=250$ kpc). The enhancement was at the $\simeq 10\%$ level and resulted from the fact that the R00 luminosity method will over estimate the true luminosity if the true core radius is smaller than the assumed value of $r_c=250$ kpc. Similar enhancements were found when R00 compared the Bright SHARC luminosities to those derived by Vikhlinin et al. (1998) for the 11 clusters they had in common. (Vikhlinin et al. 1998 used the best fit value of r_c to compute cluster luminosities and, in the majority of cases, their r_c values were smaller than 250 kpc.)

4 Areal Coverage

To be able to compute an CXLF, we need, in addition to the results of our simulations, an estimate of the area covered by the Bright SHARC survey. R00 calculated the maximum areal coverage of the survey to be 179 deg^2 . However, the R00 calculation did not include an uncertainty estimate or a quantification of how the areal coverage falls off with cluster flux. We have corrected for those shortcomings here and the results are shown in Fig. 1. Details are given in Adami et al. (2000).

5 Influence of the Different Sets of Parameters on the CXLF

Nichol et al, (1999: N99) used a preliminary set of selection function simulations to derive the Bright SHARC CXLF. This preliminary set used the same parameters as run 1, i.e. an isothermal β profile with $\beta = 0.67$, $r_c = 250$ kpc, $e = 0.15$, $\Omega_0 = 1$ and $\Omega_\Lambda = 0$, but covered a smaller range of redshifts and luminosities. Here we redetermine the Bright SHARC CXLF using the results of run 1 in order to test the robustness of the N99 results. We also investigate how the CXLF changes when we use selection functions derived from the results of runs 2 to 12. We note that we have detected a systematic trend affecting the accuracy of the Bright SHARC cluster luminosity measurements only when we use a low value of the slope β or strong cooling flow profiles (which are not, however, very likely at high redshift). None of the other tested parameters have a systematic effect. This means that our luminosity measurements are not very dependent of the parameters tested in this work.

We have used the same $1/V_a$ methodology as N99 (adapted where necessary for different cosmological models) to determine the Bright SHARC CXLF. V_a is defined as the available sampled volume for any given cluster in the survey and can be computed for a cluster of luminosity L_x using

$$V_a = \int_{z_{low}}^{z_{high}} \Omega(L_x, z) V(z) dz, \quad (1)$$

where z_{low} and z_{high} are the lower and upper bounds of the redshift shell of interest, $V(z)$ is the volume per unit solid angle for that redshift shell and $\Omega(L_x, z)$ is the effective area of the Bright SHARC survey. This effective area was calculated by multiplying the areal coverage

of the survey at the corresponding ROSAT flux by the appropriate *Bright SHARC detection efficiency*. The detection efficiency is a function of the cluster redshift and luminosity. The effective area is also (see Figure 1 for an illustration of how $\Omega(L_x, z)$ varies with L_x and z). Very bright clusters (e.g. $L_{44}=10.0$ clusters at $z = 0.25$) will have an effective area equal to the maximum areal coverage of the survey (i.e. 179 deg^2). Whereas very faint clusters will have an effective area that approaches zero.

In order to compare with the earlier calculations of N99, we show in Figure 1 the effective area computed for the standard set of parameters. The results are similar to the preliminary simulations presented in N99 except for the high luminosity and high redshift clusters, where we now find a lower effective area than thought. This is primarily due to the increased precision of the simulations presented herein. The main consequence of this change is in the statistical significance of any proposed deficit of high luminosity, high redshift clusters (see N99). We have repeated the analysis of N99 and find that at $L_x > 5 \times 10^{44}$, and in the redshift range $0.3 < z < 0.7$, we would expect to have detected about 2 clusters (using the De Grandi et al. 1999 or Ebeling et al. 1997 luminosity function) in the Bright SHARC using the effective area curves presented in Figure 1.

In N99, the CXLF was calculated using the 12 Bright SHARC clusters with $z > 0.3$. In this study we used a slightly lower redshift limit ($z > 0.285$) to increase the number of clusters in the sample. Because the simulations covered only discrete values of L_x and z , we had to use linear interpolation to estimate the detection efficiency for these clusters. The detection efficiency can vary dramatically with the run number. We did not include clusters for which the mean (over all runs 1 to 11) *Bright SHARC detection efficiency* was less than 5%. We, therefore, excluded two clusters (RXJ1334 and RXJ1308 which were both used in N99) from our list of fifteen. The remaining thirteen clusters are divided into 4 luminosity bins (see Fig. 2). These bins contained 4, 5, 3 and 1 clusters respectively. The redshift ranges for these bins were slightly different from N99; for bins 1,2 and 3 we used $0.285 \leq z \leq 0.7$ (compared to $0.3 \leq z \leq 0.7$) and for bin 4 we used $0.285 \leq z \leq 1.0$ (compared to $0.3 \leq z \leq 1.0$).

The results are shown in Figure 2. In this figure, we have overplotted the local CXLF computed by de Grandi et al. (1999) and Ebeling et al. (1997).

We present 4 separate sets of CXLF results, comparing the run 1 number densities to those derived from runs 4 through 12. We see, from the lower left panel, that ellipticity has a very small effect on the CXLF. However, in the other 3 panels we see some quite dramatic effects when we change the core radius (lower right panel), the value of β (upper left panel) and surface brightness profile (upper right panel: we have only plotted the results using moderate cooling flows and NFW profiles). When clusters are more diffuse (e.g. if β is smaller or r_c is larger than our canonical values), the detection efficiency declines hence the cluster number density goes up. By contrast, when the clusters become more concentrated (e.g. if we use a NFW profile or a strong cooling flow instead of an isothermal β model), then detection efficiency goes up and the number density goes down.

In summary, we have shown that the N99 CXLF is robust, under the assumption of standard parameters, despite the fact that it was derived using a less sophisticated set of selection function simulations than run 1. We find that the CXLF is not very sensitive to the values of certain parameters, Ω_0 , Ω_Λ and ellipticity. Other parameters have a more significant effect on the CXLF; these are the values of β and r_c and the shape of the cluster surface brightness profile. If all clusters had NFW profiles, for example, then the N99 CXLF will significantly over estimate the number density of high redshift clusters (since it was derived using a selection function that assumed isothermal β profiles). Alternatively, if all clusters had large core radii, then the N99 CXLF will significantly under estimate the number density of clusters (since it was derived using a selection function that assumed $r_c = 250 \text{ kpc}$).

6 Discussion

The evolution of the CXLF with redshift, especially at the bright (i.e. high mass) end, provides - in principle - strong constraints on the value of Ω_m . If we see, for example, a much lower number density of high luminosity clusters at high redshift, as opposed to the number density at low redshift, then we have strong support for a high Ω_m Universe (and vice versa) because Ω_Λ has little effect on the evolution of the CXLF out to at least $z \sim 1$ (e.g. Holder et al. 2000). However, since the existing cluster samples only contain very small numbers of distant and luminous clusters, our ability to constrain Ω_m crucially depends on our ability to define the volume in which those clusters were detected. For example, the Bright SHARC has only one cluster in the highest luminosity bin (RXJ0152). If we over (under) estimate the volume in which this cluster was detected then our number density will be too low (high) and our inferred value of Ω_0 too high (low).

We attempted to determine the sensitivity of the Bright SHARC CXLF to the assumptions that were incorporated into the selection function simulations. We have shown that the initial choice of cosmological parameters has only a small influence on the CXLF. This result is fundamental because it means that, whatever cosmology is assumed when measuring the CXLF, we will still be able to probe CXLF evolution, and thus constrain the value of Ω_m . The same cannot be said for the assumed surface brightness model; if all clusters follow NFW profiles or have strong cooling flows, we will significantly over-estimate the high z cluster number density (and thus drive Ω_m down). By contrast, if we underestimate the value of r_c , or overestimate the value of β , we will significantly underestimate the high z cluster number density (and thus drive Ω_m up).

With the X-ray data currently available we are not able to quantify just how much the various selection function assumptions might bias an Ω_m measurement. This is because we are not able to determine the distribution of r_c and β values for the Bright SHARC clusters, or determine what fraction of those clusters are better fit with NFW profiles than with isothermal β profiles (see also Durret et al. 1994). To address this, we have begun a program to study cluster morphologies (and temperature profiles) with the new X-ray satellites XMM and *Chandra*. The follow-up of known clusters, such as those in the EMSS or Bright SHARC samples, will be one of major contributions of XMM and *Chandra* to cosmology. Both satellites have smaller fields of view than did ROSAT and so do not lend themselves well to serendipitous, or dedicated, cluster surveys. The catalogs derived from the ROSAT archive (see also Ebeling et al. 2000) will remain the pre-eminent source of high redshift X-ray clusters for some time to come. The recent work by Romer et al. (2000b) has demonstrated that in 5-10 years, XMM will have covered sufficient area to sufficient depth to allow new cluster catalogs to be created. These new catalogs will contain more high redshift, high luminosity clusters than the ROSAT and EMSS samples and so will provide much better constraints on Ω_m . These catalogs will require detailed simulations in order to determine their selection function. The work presented herein provides important guidelines as to how those simulations should be carried out.

Previously, several other groups (e.g. Vikhlinin et al. 1998, Burke et al. 1997, Scharf et al. 1997 or Rosati et al. 1995) have simulated selection functions in order to measure their CXLF's. Their methods were generally the same as those in this paper. All the morphological parameters tested here were, however, not included, preventing them from showing the dependence of the selection function with the X-ray morphology of the clusters. In a future work we plan to apply our results to the faint SHARC sample (including the Southern SHARC by Burke et al. 1997) and to derive the limits to the evolution of the CXLF based on the uncertainties we have determined.

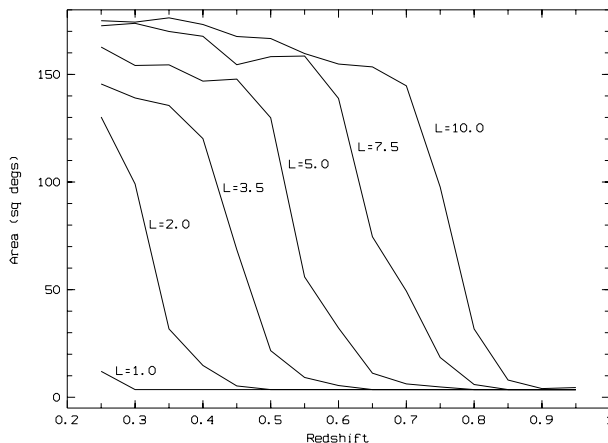


Figure 1: Effective area of the Bright sample as a function of cluster luminosity and redshift. The six curves represent the six different input luminosities (in units of 10^{44} ergs.s $^{-1}$).

7 Summary and Conclusions

The areal coverage of serendipitous surveys, such as SHARC is, as we have shown here, poorly determined at faint flux limits. For the Bright SHARC CXLF we have demonstrated that all the clusters in this sample are bright enough that the error in the areal coverage is $\sim 5\%$. The uncertainty of the completeness of the survey then, becomes important when the areal coverage uncertainty is so small.

We have carried out a detailed set of simulations in order to probe the effects of certain assumptions about distant clusters and the geometry of the Universe on the completeness of the Bright SHARC survey. These assumptions have ramifications for the Cluster X-ray Luminosity Function (CXLF) derived for the SHARC survey and, ultimately, for the value of the matter density (Ω_m) derived from CXLF evolution. Under the assumption of a standard set of morphological parameters, we find that the Bright SHARC CXLF as determined by N99 (using a less sophisticated set of selection function simulations) is robust. The new Bright SHARC CXLF presented in Figure 2 agrees (within the 1 sigma envelope) with earlier estimates of the SHARC CXLF (Nichol et al. 1997, N99, Burke et al. 1997) and shows no statistical evidence for strong evolution at any luminosity out to $z=0.7$. At present, we are unable to make any definitive statement about a possible deficit of high redshift, high luminosity clusters in the Bright SHARC (see N99) since we are still hampered by a combination of small number statistics, uncertainties in the local CXLF, incompleteness in our optical and X-ray follow-up as well as the systematic uncertainties in the Bright SHARC selection due to the unknown surface brightness profiles of distant clusters.

We find that certain assumptions have little effect on the detection efficiency of the survey: the moderate ($e \leq 0.3$) ellipticity of the cluster or the presence of moderate cooling flows. None of these assumptions has a significant impact on our ability to measure cluster luminosities using the simple method adopted in R00. Other assumptions, specifically those associated with the cluster X-ray morphology (e.g. sharply peaked surface brightness profile or high ellipticity), can have a significant impact on cluster detectability (and the inferred completeness of the survey) and the derived CXLF. We have shown, then, that even with an increased number of detected clusters, the results based on attempting to measure CXLF evolution to constrain Ω_m will remain highly uncertain. Follow-up studies by *Chandra* and XMM that measure the X-ray morphology of distant clusters will, therefore, play a key role in the measurement of Ω_m .

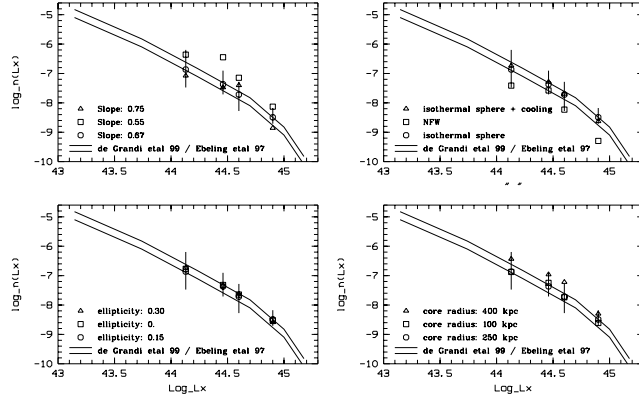


Figure 2: The Bright SHARC CXLF as a function of cluster morphology: (lower left) ellipticity ; (lower right) core radius ; (upper left) slope β ; (upper right) surface brightness profile. The x-axis gives the log of the cluster luminosity (erg s^{-1}) in the [0.5-2.0 keV] band. The y-axis gives the log of cluster number density in units of $\text{Mpc}^{-3} (10^{44} \text{ erg s}^{-1})^{-1}$. The error bars are shown for the run 1 points (circles). The two solid lines are the envelope of the local CXLF from De Grandi et al. (1999) and Ebeling et al. (1997).

References

1. Adami, C., et al., 2000, ApJS 131
2. Bahcall, N.A., Fan, X., & Cen, R. 1997, ApJ, 485, L53
3. Borgani, S., Rosati, P., Tozzi, P., & Norman, C. 1999, ApJ, 517, 40
4. Burke, D.J., Collins, C.A., Sharples, R.M., Romer, A.K., Holden, B.P., & Nichol, R.C. 1997, ApJ, 488, L83
5. Durret, F., Gerbal, D., Lachieze-Rey, M., Lima-Neto, G., & Sadat, R. 1994, A&A, 287, 733
6. Ebeling, H., Edge, A., & Henry, J.P. 2000, Large-Scale Structure in the X-ray Universe, Plionis & Georgantopoulos (eds), atlantisciences, p39
7. Ebeling, H., Edge, A.C., Fabian, A.C., Allen, S.W., Crawford, C.S., & Bohringer, H. 1997, ApJ, 479, L101
8. de Grandi, S., Bohringer, H., Guzzo, L., Molendi, S., Chincarini, G., Collins, C., Cruddace, R., Neumann, D., Schindler, S., Schuecker, P., & Voges, W. 1999, ApJ, in press
9. Gunn, J.E., & Gott, J.R. 1972, ApJ, 176, 1
10. Henry, J.P., Gioia, I.M., Mullis, C.R., Clowe, D.I., Luppino, G.A., Böhringer, H., Briel, U.G., Voges, W., & Huchra, J.P. 1997, AJ, 114, 1293
11. Henry, J.P., & Henriksen, M.J. 1986, ApJ, 301, 689
12. Holder, G.P., Mohr, J.J., Carlstrom, J.E., Evrard, A.E., & Leitch, E.M. 2000, ApJ submitted
13. Lacey, C., & Cole, S. 1993, MNRAS, 262, 627
14. Navarro, J.F., Frenk, C.S., & White, S.D.M. 1997, ApJ, 490, 493
15. Nichol, R.C., Romer, A.K., Holden, B.P., Ulmer, M.P., Pildis, R.A., Adami, C., Merrelli, A.J., Burke, D.J., & Collins, C.A. 1999, ApJ let, 521, L21: N99
16. Oukbir, J., & Blanchard, A. 1997, A&A, 317, 1
17. Oukbir, J., & Blanchard, A. 1992, A&A, 262, L21
18. Peres, C.B., Fabian, A.C., Edge, A.C., et al. 1998, MNRAS, 298, 416
19. Press, W.H., & Schechter, P. 1974, ApJ, 187, 425
20. Reichart, D.E., Nichol, R.C., Castander, F.J., Burke, D.J., Romer, A.K., Holden, B.P., Collins, C.A., & Ulmer, M.P. 1999, ApJ, 518, 521

21. Richstone, D., Loeb, A., & Turner, E.L. 1992, ApJ, 393, 477
22. Romer, A.K., Viana, P., Liddle, A., & Mann, R.G. 2000b, ApJ, in preparation
23. Romer, A.K., Nichol, R.C., Holden, B.P., Ulmer M.P., Pildis, R.A., Merrelli, A.J., Adami, C., Burke, D.J., Collins, C.A., Metevier, A.J., Kron, R., & Commons, K. 2000a, ApJS in press: R00
24. Rosati, P., Della Ceca, R., Burg, R., Norman, C., & Giacconi, R. 1995, ApJ, 445, L11
25. Sadat, R. 1998, ApSS, 261, 331
26. Scharf, C.A., Jones, L.R., Ebeling, H., Perlman, E., Malkan, M., & Wegner, G. 1997, ApJ, 477, 79
27. Viana, P.T.P., & Liddle, A.R. 1999, MNRAS, 303, 535
28. Viana, P.T.P., & Liddle, A.R. 1996, MNRAS, 281, 323
29. Vikhlinin, A., McNamara, B.R., Forman, W., Jones, C., Quintana, H., & Hornstrup, A. 1998, ApJ, 502, 558